

# UC Berkeley

## UC Berkeley Previously Published Works

### Title

Simulation and power quality analysis of a Loose-Coupled bipolar DC microgrid in an office building

### Permalink

<https://escholarship.org/uc/item/416851bp>

### Authors

Wang, Ruiting

Feng, Wei

Xue, Huijie

et al.

### Publication Date

2021-12-01

### DOI

10.1016/j.apenergy.2021.117606

### Copyright Information

This work is made available under the terms of a Creative Commons Attribution-NonCommercial License, available at <https://creativecommons.org/licenses/by-nc/4.0/>

Peer reviewed

# Simulation and Power Quality Analysis of a Loose-Coupled Bipolar DC

## Microgrid in an Office Building

Ruiting Wang<sup>a, b</sup>, Wei Feng<sup>b \*1</sup>, Huijie Xue<sup>b, c \*2</sup>, Daniel Gerber<sup>b</sup>, Yutong Li<sup>d</sup>, Bin Hao<sup>d</sup>, Yibo Wang<sup>e</sup>

a, University of California Berkeley, Berkeley, CA 94720, USA

b, Lawrence Berkeley National Laboratory, Berkeley, CA 94720, USA

c, Beijing University of Civil Engineering and Architecture, Beijing, China P. R. 100044

d, Shenzhen Institute of Building Research, Shenzhen, Guangdong Province, China P. R.  
518049

e, Institute of Electrical Engineering, Chinese Academy of Sciences, Beijing, China P. R.  
100190

\* Corresponding author 1: MS2021, 1 Cyclotron Road, Berkeley, CA 94530. Email:

weifeng@lbl.gov

\* Corresponding author 2: No.1 Zhanlanguan Road, Xicheng District, Beijing, China, 100044.

Email: xuehuijie@bucea.edu.cn

## **Abstract**

With distributed generation and battery storage technologies thriving in microgrids, the use of direct current (DC) microgrids in the building sector offers multiple advantages in energy efficiency and power quality compared with alternating current (AC) systems. This study developed a new concept of a loose-coupled bipolar DC building power system. The concept was used to design a real-world office building in Shenzhen, China. A power system simulation model was developed to study the stability and control of the DC power system and maintain DC power quality. The design of the DC power control system is discussed and modeled to maintain the power system's stability. Using the designed control system, the study developed a few common fault scenarios in DC building microgrids, and the fault scenarios were simulated in the MATLAB-Simulink environment to validate the design of a loose-coupled bipolar DC system. The results indicate that the loose-coupled bipolar DC system schema, when implemented with proper control algorithms, can achieve good fault-tolerant performance with reliable power quality, even during disruptive system events.

## **Keywords**

DC power, Bipolar, Microgrid, Simulation, Stability

## 1. Introduction

The dominance of AC systems in various electrical power distribution and transmission has been the market status quo since the origin of electrical current. The prevailing system was mainly built and developed at a time that nearly all generating and end-use systems were for AC power [1], and when affordable DC/DC converters were unavailable. However, recent decades have seen the development of economical and efficient DC/DC converters, DC-based power generation sources, and an ever-increasing number of DC-consuming devices and loads. This includes environmentally friendly energy resources such as solar photovoltaics (PV) and fuel cells, as well as DC-based end uses in buildings, such as light-emitting diodes (LED) and a variety of electronics [2] such as computers and televisions. Under this context, the application of DC in distribution appears to be advantageous from multiple aspects.

In terms of energy efficiency, the use of DC components in combination with the AC/DC power converters results in energy loss and decreases building power system efficiency. Up to 13% of the electricity lost in commercial office buildings comes from distribution and conversion [3]. With the progress of building-level microgrid systems, more studies have revealed that DC power distribution systems combined with enablers like generation, energy conversion, storage, and load control have great energy saving potentials [4]. DC microgrids are also reported to have better power quality, but they also have their own distinctive power quality issues apart from AC microgrids. Barros et al. [5] and Rawat et al. [6] summarized the most common potential power quality issues in DC microgrids, and these will be discussed further in Chapter 2.2. To summarize, DC microgrids are advantageous, but they need careful

design and proper control to maximize their benefit and to avoid potential problems.

Although the use of DC microgrids in buildings is a relatively new concept, some power systems, including spacecraft, data centers, and telecommunications, typically employ DC distribution. A NASA/ASEE Summer Faculty Fellowship Program in 1994 simulated high-voltage, high-power DC distribution systems in spacecraft with steady-state models of each component [7]. DC distribution systems in spacecraft involve a large number of PV arrays, DC/DC converters, battery storage systems, and DC loads [8]. In data centers, DC distribution can be used to reduce energy loss. Duke Energy and the Electric Power Research Institute (EPRI) found that a DC microgrid system cut energy consumption up to 15% compared to a typical AC system with a double-conversion uninterruptible power supply (UPS) [9]. Thompson et al. developed voltage stabilization control in telecommunications DC distribution systems [10]. The wide utilization and multiple benefits of DC microgrids indicate the great potential such a system has in further development in buildings.

There are two conventional ways to transmit power in DC building microgrid. The 2-wire unipolar system offers only one voltage level; the 3-wire bipolar system can offer two voltage levels, with a positive wire, a negative wire, and a neutral wire. Compared to a unipolar system, a traditional bipolar system (Figure 1a) usually has higher energy efficiency [11]. Yet, in traditional bipolar systems, the asymmetrical loading in the positive and negative poles results in the unbalanced voltage across the bipolar microgrid, which is not desired due to its impact on power quality and energy efficiency. Meanwhile, the unequal voltage drop also leads to current flowing in the N-line, and causes corrosion [12]. A detailed introduction and

comparison of the unipolar system and traditional bipolar system was given in Chapter 2.3, Building Microgrid Polarity, in the literature review. To avoid the voltage unbalance issue in traditional bipolar systems, this study developed a comprehensive building-scale DC power simulation model with a loose-coupled bipolar system (Figure 1b), with a real setup of a building in Shenzhen, China.

The loose-coupled bipolar system proposed by this research consists of two power poles. The positive and negative poles are controlled separately and coupled with a common neutral line. In contrast to a traditional bipolar system, in a loose-coupled bipolar system, the function of each pole does not affect the other pole. In other words, from a control point of view, the loose-coupled system can be treated as two separate single-pole systems. However, the two poles are coupled in the sense that they share one neutral line and that the DC power system can operate at a single-pole voltage level or combine both poles and operate at a high voltage level. Figure 1 demonstrates the comparison of AC/DC conversion topology of traditional bipolar and loose-coupled bipolar DC microgrids.

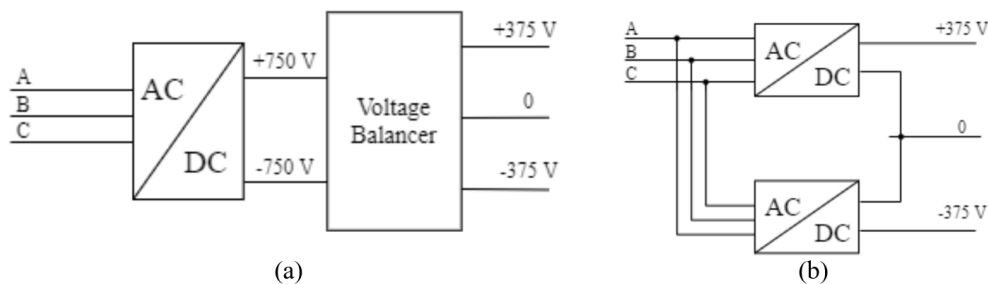


**Figure 1. AC/DC topology in (a) a bipolar system, and (b) a loose-coupled bipolar system**

These characteristics give building microgrids the robustness to operate in different voltage

levels based on the end-use equipment requirements. For example, compressor-based equipment such as air-conditioners can utilize both poles and operate at a relatively higher voltage level, while other low voltage appliances can be fed directly through each pole's power electronics devices. Another advantage of a loose-coupled bipolar system is the enhancement of building power system robustness. In traditional bipolar systems, a fault introduced into one pole may affect the power electric devices on the other pole and thus influence the performance. Unlike those in traditional bipolar systems, faults introduced into the loose-coupled bipolar microgrid can be isolated successfully through the bipolar structure as well as at different levels of power electronic devices. Hence, a fault introduced at a location can be successfully contained and will not propagate to the entire building microgrid system.

This study analyzes DC power system performance with a focus on system stability and control by developing several scenarios in building grid-connected mode and island operation mode. The goal of the controller design is to maintain the stability of the DC building system, and the performance of the controller was exhibited through scenario simulations. The main contributions of this study are:

- (1) It defined and developed a well-performed loose-coupled bipolar system topology in buildings.
- (2) It used a real case study and developed a generic loose-coupled bipolar DC power simulation framework.

(3) It simulated a few DC building power system disruptive scenarios to validate the control strategy performance, operating stability, and robustness of DC microgrids.

The paper is structured as follows: Section 2 presents a literature review regarding multiple topics related to building DC distribution system design; Section 3 introduces the methodology used in designing and modeling of electronic components and the system; Section 4 presents the results of system stability and robustness tests under different scenarios in the dynamic model; and Section 5 discusses the overall performance, future applications, and conclusions.

## **2. Literature Review**

Several important topics about the design of DC microgrids in the building were reviewed to build a bigger picture of the application of DC microgrids in buildings, as well as the advantages and disadvantages of this issue. This section first covers the existing studies of energy saving potential and power quality in DC microgrids, as well as characteristics of bipolar microgrids. It then explores different control strategies in the converter and the droop control. Section 2.5 details the scope, contribution, and uniqueness of this study.

### **2.1 Benefit of DC microgrids: Energy saving potential**

Many demonstration projects and case studies focus on the energy-saving potential of DC distribution systems compared to AC systems, both by the experimental method [13–15] and by simulation [2–4,16–19]. For commercial buildings, the reported savings vary from 2% [13] to 19% [18], depending on the different experimental mock-up. Generally, the systems with

batteries and PV arrays have higher saving potential, and the overall saving is highly dependent on the efficiency of AC/DC converters [1], DC distribution system topology, and voltage level, as well as the coincidence of loads with PV generation [16]. Differences also exist in different scales of modeling cases and experimental cases. Boeke and Wendt [13] measured an efficiency advantage of 2% with a small DC grid testbed and in a higher power level, and estimated a saving potential of 5%. Electric energy savings of 5%~8% using a DC system without battery storage systems were found [2][5]; and in the case of a battery storage system, the savings could be up to 13%~14% [3][16]. The energy-savings potential measured in experiments varies from 2% to 8% in different cases with no battery storage [13–15]. Most of these models in existing studies have employed simple simulation setups, or used simplified experimental setups to build the model. This approach caused different results of the quantified potential savings of DC microgrids, and therefore, there is a need for more detailed simulations validated by experimental data. To understand the different characteristics of building electric and energy systems, modeling approaches with different time steps have been developed. Energy-saving potential has usually been simulated using a static-state model with a longer time step, such as a 15-minute or hour time interval. In contrast, to evaluate power quality and conduct DC system control and stability analysis, shorter time steps are required to capture the dynamic feature of DC power systems.

## **2.2 Benefit of DC microgrids: Power quality**

DC microgrids are not only more cost-effective in the sense of their energy-saving potential, they also provide better power quality [6]. Power distribution through DC frees the system

from AC harmonics. Reviews of existing DC microgrid power quality standards, definitions, and international regulations were made in [5,20], and they also note that the development of the definition and standardization of supplied voltage and power quality generally fall behind the growing need. With tightly controlled DC voltage, DC microgrids are recognized as more tolerant against AC side disturbances [21]. Different DC microgrids components have different voltage characteristics. Technologies like PV arrays and battery storage by themselves can produce ideal or quasi-ideal DC voltage; however, AC/DC and DC/DC converters produce DC voltage with ripple content [5]. Thus, voltage stability becomes an important feature of power quality in DC microgrids. It requires a more attentive design of AC/DC or DC/DC converters. Many studies regarding power quality focus on solutions to specific power quality issues. For example, [22] used active damping to improve the stability of DC grids when the number of solar power optimizers increases; [23] implemented nonlinear control to deal with negative impedance instability that occurs in constant power loads; and [24] applied converter interleaving to reduce the voltage ripple and improve efficiency. Nevertheless, most studies used simplified models. To the authors' best knowledge, no study has conducted simulations on a full-scale building using real setups with detailed dynamics and possible operational situations. It was the main focus of this study to perform a building-scale detailed model analysis so the actual performance of DC microgrids and DC distribution systems could be analyzed and verified.

### **2.3 Building microgrid polarity**

There are two conventional ways of power-transmitting in DC building microgrids: either

through a 2-wire unipolar system or a 3-wire bipolar system with an additional neutral wire. In 2010, Kakigano, Miura, and Ise first proposed and defined a “low-voltage bipolar-type dc microgrid,” where DC power is distributed through 3-wire lines [25]. The sketch of this configuration also appeared in their former works [26,27]. A bipolar DC distribution network is considered the counterpart of a three-phase AC distribution network [28]. Bipolar systems are generally regarded as more energy-efficient than unipolar systems while improving supply reliability [11]. Compared to a 2-wire unipolar system, a traditional bipolar DC system allows distribution networks to transfer twice the amount of power with lower conduction losses, while being able to provide two voltage levels: pole-to-pole, and pole-to-neutral. It offers more options to DC devices suitable for different voltage levels and further reduces the energy loss due to potential voltage conversion [25]. However, it also should be noted that, in a traditional bipolar systems, an unbalanced load or generation distribution between positive-neutral or negative-neutral lines can cause the voltage to be unbalanced and lead to non-zero neutral conductor currents [29], which increases feeder losses and can cause system instability. In response to this potential risk, literature has promoted voltage balancers or switchovers that can reconfigure DC loads to either pole. [11] made a comprehensive analysis of voltage balancers and also proposed the topology deduction method; [30] introduced a DC electric spring to balance the unbalanced power flow and reduce energy losses due to neutral line currents. Combining the advantages of both, this study proposes a loosely-coupled bipolar system. The system retains the advantageous 3-wire system of a bipolar DC microgrid, being able to provide multiple voltage levels and reduce energy losses. It also eliminates the drawbacks of possible voltage unbalance and non-zero neutral conductor currents.

## **2.4 DC system power electronics control**

Power converters are crucial components in AC and DC distributions. For DC building microgrids, DC/DC converters play an equally important role as AC/DC converters. Compared to an AC/DC converter, where a power factor correction is required to decrease the loss in parasitic resistance related to the reactive power and improve the capacity utilization rate of the power equipment, the DC/DC converter is naturally more efficient. Today's DC/DC converters can achieve efficiencies of 98% or higher using some additional techniques [16], making them more energy-efficient for DC building microgrids.

To achieve beneficial improvement of power quality on DC microgrids as mentioned, precise control of the converters is needed. This section covers popular DC system power electronics control methods, some of which were adopted in our simulation.

### **2.4.1 AC/DC, DC/DC converter control**

Generally, there are two types of control methods in converters—voltage source control and current source control converters—both of which are commonly used in DC microgrids. To maintain better power quality, numerous control strategies have been developed: a classical linear control system with feedback or feedforward loops [31–34]; multiple nonlinear controls, including sliding mode control [35]; a feedback linearization control [36]; a Lyapunov-based control [37]; and others. These control strategies are designed to improve system stability under adverse scenarios.

Although nonlinear control methods exert superiority in certain aspects, like transient

response and stability, the complex computations and parametric sensitivities of these methods sometimes limit their utilization [38]. In this model, both primary control strategies and secondary distributed control were taken into consideration, to maintain system stability.

#### 2.4.2 Droop control

Droop control parallelizes multiple sources controlling the voltage in a DC microgrid, which is critical for stabilizing the DC microgrid and prevents a single-point-of-failure. Droop control has been widely used in cases of adjusting load sharing because it does not require communication lines, which provides high reliability and has a relatively simple topology [39]. In most cases, droop control brings a “virtual resistance” into the existing system. In contrast to real resistance, the “virtual resistance” produces no “real” power loss and is unaffected by changes in working conditions, such as temperature. Droop control is also known as *droop gain*, *droop constant*, or *droop coefficient* [40].

Droop control was first developed in AC systems. In an inductive system, the active power drawn to the bus from the inverter is predominantly dependent on the power angle, while the reactive power is mainly determined by AC voltage. Since the inverter output voltage phase can be dynamically influenced by voltage frequency, the wireless control primarily uses frequency droop and output voltage droop [41]. The characteristics of  $P$ - $f$  and  $Q$ - $V$  droops in AC systems could be described by the following equations:

$$\begin{aligned}\omega &= \omega^* - k_{P-f}(P - P^*) \\ V &= V^* - k_{Q-V}(Q - Q^*)\end{aligned}\tag{1}$$

where  $\omega$  and  $V$  stand for the frequency and amplitude of output voltage;  $P$  and  $Q$  are the active and reactive power measurement;  $k_{Q-V}$  represents the  $P$ - $f$  and  $Q$ - $V$  droop; and characters with \* stand for the references of each measurement.

The same concept has been adapted to DC systems. Given that in DC microgrids DC power can be decided by voltage only, the concept of “reactive power” is no longer applicable, and only “active power” is transferred in the line. A relationship between active power  $P$  and DC voltage  $V$  is built in this case.

The concept of droop control in DC microgrids is mainly divided into two categories: current/power mode droop and voltage-mode droop [42]. Under voltage control mode, the voltage reference is set, and the converter operates as a controllable voltage source. Likewise, converters under current/power mode control operate as a controllable current/power source, with the output current/power regulated by the set references. Taking voltage mode as an example, the reference voltage is generated according to voltage droop and the branch output DC using the  $V$ - $I$  droop characteristics:

$$V_{dc}^* = V_o - I_{dc}k \quad (2)$$

where  $V_o$  is the nominal bus voltage;  $k$  is the virtual resistance or droop gain;  $I_{dc}$  is the DC measurement; and  $V_{dc}^*$  is the generated DC voltage reference [43].

With multiple power sources, droop control is necessary to guarantee load-sharing performance. In off-grid mode, where the grid cannot regulate the power bus, there is a possibility of multiple generation sources sharing loads. In order to ensure that load sharing is

appropriate and efficient, voltage droop control is utilized in AC/DC converters and DC/DC converters connecting the energy storage system (ESS) and the main bus. ESS supplies energy to the system in islanded mode and plays a role in peak cutting. Virtual resistance is decided by the measured current level, as well as different source voltage.

## **2.5 Uniqueness of this study**

The aforementioned literature has comprehensively studied the performance and characteristics of insular components in the DC microgrids, but the simulation and modeling are mainly confined to a component level to highlight the performance of the specific individual components in a DC power system.

Few studies have focused on the overall performance of a whole building system, and the building-level DC power system simulation cases capturing variable scenarios of system stability performance have not been comprehensively studied. Very little research has studied the design and operation of DC power systems or the power system stability of building-scale DC microgrids. No existing studies have raised the issue of design and operation of loose-coupled bipolar system buildings. More detailed and integrated simulation based on a real building setup is needed to evaluate DC building power system performance with the up-to-date technologies commonly found in the DC microgrids.

This study developed a dynamic model to evaluate power quality in different scenarios for DC power systems in buildings. It exhibited through a case study how to design and control a DC power system to enhance system stability.

### **3. Methodology**

#### **3.1 Building DC power system configuration**

The building studied is located in Shenzhen, China, which belongs to the Subtropical Monsoon Climate and has warm and humid summers with a lot of rain and relatively dry winters. It is a six-floor commercial building with a total floor space of 5,000 square meters (m<sup>2</sup>). The DC microgrid system consists of a PV array, battery storage, multiple DC voltage buses, various DC loads, and AC/DC and DC/DC converters.

The building has three bus voltage levels: 750 volts (V), 375 V, and 48V. The total capacity of the building is 311.8 kilowatts (kW), which includes a 60 kW DC charging pile for electric vehicles (EV) and a 50 kW centralized ESS. The building also has a 75 kW PV array on each pole, providing a total power of 150 kW. Compared to a unipolar system, this loose-coupled bipolar system provides two levels of voltage in the main power bus: a positive-neutral or negative-neutral voltage level of +/-375 V and a positive-negative voltage level of 750 V.

The system consists of two power conversion processes: one at a grid-tied conversion that can bidirectionally convert grid AC power to the bipolar plus and minus DC voltage level bus bar, and another at the end-user level, to conduct a DC-DC power electronics conversion. Figure 2 shows a detailed schematic design of the building.

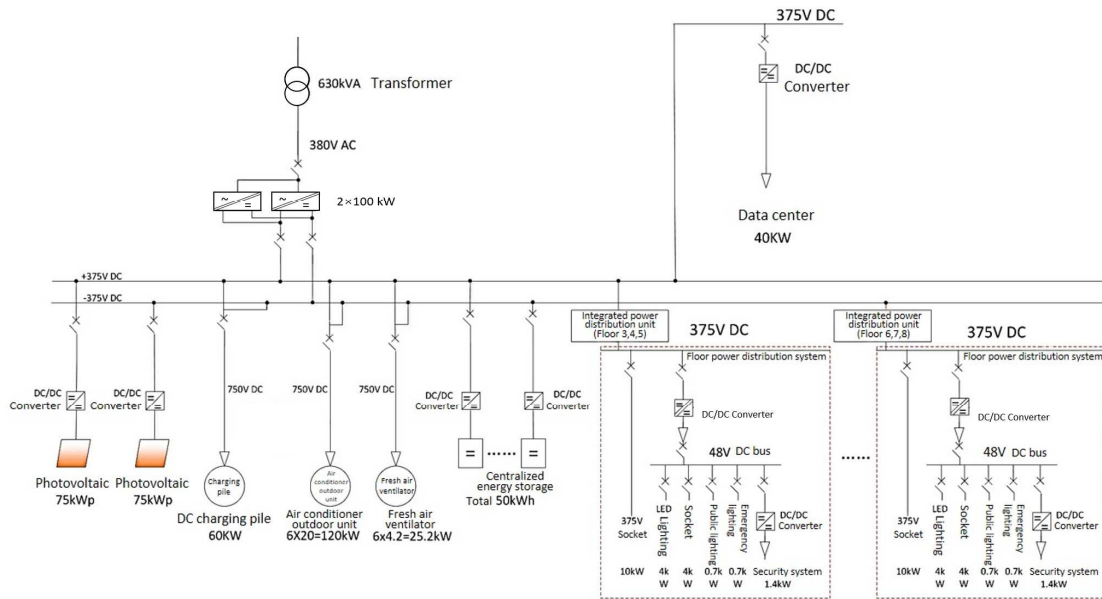


**Figure 2. DC building microgrid design schematic**

The PV array, centralized energy storage, and a 40-kW data center are connected to the 375 V DC voltage bus; the DC charging pile for EVs, a variable refrigerant flow air-conditioning system, and a fresh air ventilator are powered by 750 V DC power. In this six-floor office building, the positive and negative line was symmetrically arranged on the adjacent floor to maintain the power consumption at the +/- 375 V power bus at roughly the same level. Floors 1, 2, are elevated open parking spaces without electric loads. Floor 3, 5, and 7, and floors 4, 6, and 8 were connected with the +375 V power bus and -375 V power bus, respectively. A low voltage DC bus used to feed local power use such as lighting, plug loads, and other DC consuming devices was designed as 48 V at floor level. DC/DC converters were used on each floor to convert the power voltage level from 375 V to 48V.

Two types of grounding methods are considered in the DC microgrid building system. Both IT and TNS grounding are used for the real building electrical and electronic system design. In

the IT grounding network, the distribution system is isolated from the earth. TN grounding has one point after the rectifier directly connected with the earth, and the bodies of all electrical devices are connected to the same earthing point. TNS grounding refers to a case where the PE (protective earth) and N (neutral line) are two separate conductors.

During regular operations, the neutral line is isolated from the earth. This scenario is called the *floating ground method*. The reason to use a floating ground is to avoid AC interfusing DC systems through the ground. With IT grounding, the fault current of a pole-to-earth fault is very low, which reduces the touch voltage to a safe level, but makes faults harder to detect. The system needs to consistently monitor the insulation to earth and alert when faults occur. However, insulation monitors are unable to locate the faults in the DC microgrids. Once a pole-to-earth fault is detected by the insulation monitor, the system would switch to TNS grounding and locate the faults by residual current devices (RCDs). In addition, all exposed-conductive parts and extraneous-conductive parts are connected to the same earthed point of the power supply using protective conductors.

To simulate the schematic design of the DC building microgrids, the main configuration was extracted. In Figure 3, the system includes DC loads in different voltage levels, DC generation, DC storage, and power electronic components. The outdoor unit of air conditioning is powered by the 750 V voltage bus, and the indoor unit of air conditioning is powered by the 375 V power bus.

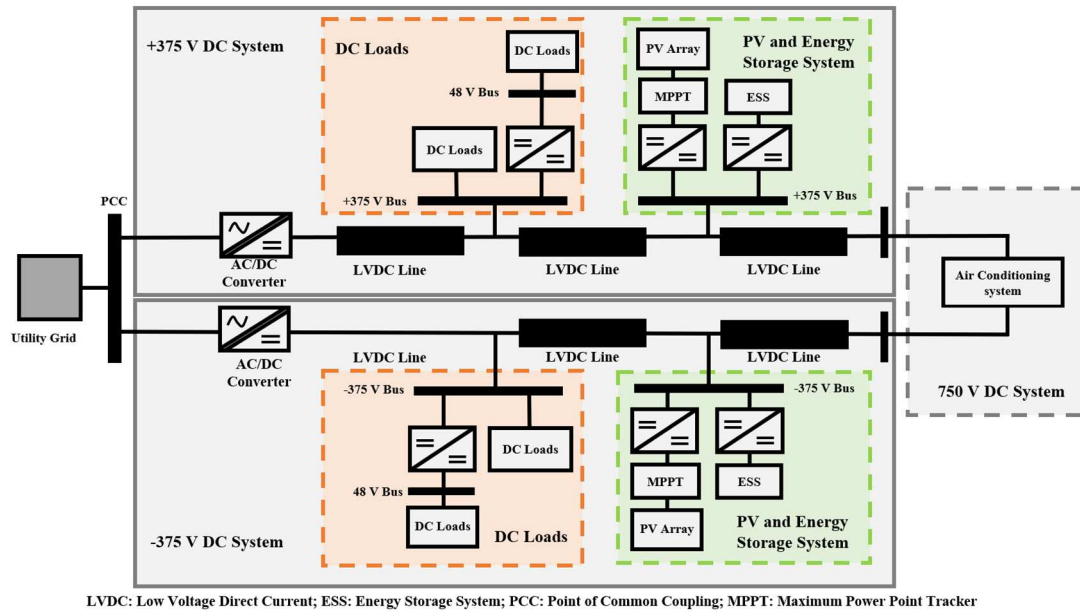


**Figure 3. DC building microgrids simulation schematic**

The DC building microgrids have two different modes of operation regarding different situations: off-grid and grid-connected. A transient power model focusing on the power quality performance and dynamic characteristics of the DC building microgrids was built in the MATLAB-Simulink environment. The model consists of multiple AC/DC and DC/DC converters, as well as components shown in the loose-coupled bipolar system DC building microgrid schematic design. The following sections will introduce the specifications of loads and the design method of the converters, and will also cover the modeling process of other components by sequence.

### 3.2 Loads and renewable generation

The model applied EnergyPlus [44] to calculate DC loads and renewable energy generation in the building based on the average historical annual climate data of Shenzhen, China. The

inputs included: building envelope characteristics, orientation, mechanical, and electrical design information. The acquisition of the characteristic load profiles and PV generation profiles was essential to determine the range of the maximum load fluctuation and the amount of load that the system needs to handle. This information was input into the dynamic characteristics modeling.

### 3.3 Design method of converters

As mentioned in Section 2.4.1, even though nonlinear control methods exert superiority in certain aspects, they can require complex computations, and their parameters are sensitive [38]. Thus, a practical and effective method based on current-mode control was used to develop the converters in this case.

The DC/DC converters in our model were designed based on literature [45–47]. The method combined peak current mode control with ramp compensation to reduce the ripples. Apart from regular buck converters and boost converters, bidirectional buck/boost converters were used to satisfy the need to charge and discharge the ESS.

The transfer function of a buck converter with a high-frequency correlation term can be described by:

$$F(s) = K \frac{1 + \frac{s}{\omega_z}}{1 + \frac{s}{\omega_p}} \cdot \frac{1}{1 + \frac{s}{\omega_n Q_p} + \frac{s^2}{\omega_n^2}} \quad (3)$$

where the dominant pole  $\omega_p$  is determined by the load resistor and capacitor, and the

transfer function zero  $\omega_z$  is determined by the equivalent series resistance of the capacitor.

The high-frequency correlation term has taken into consideration the double-pole oscillation at half the switching frequency  $\omega_n$ , the damping  $Q_p$ , the details of which can be found in [45].

Likewise, the boost converter with an additional right-half-plane (rhp) zero, expressed by  $\omega_{zrhp}$ , can be described with the following transfer function with the same nomenclature aforementioned.

$$F(s) = K \frac{\left(1 + \frac{s}{\omega_z}\right) \cdot \left(1 - \frac{s}{\omega_{zrhp}}\right)}{1 + \frac{s}{\omega_p}} \cdot \frac{1}{1 + \frac{s}{\omega_n Q_p} + \frac{s^2}{\omega_n^2}} \quad (4)$$

The ramp compensation is added when the duty cycle reaches  $D=36\%$ , an empirical value provided by [45], to make sure the current loop does not oscillate. AC/DC converters in the model were designed with proportion-integration (PI) control. These transfer functions were used in the simulation constructing process.

### 3.4 Modelling of other components

#### 3.4.1 PV generation system

An in-built library model in MATLAB-Simulink was used to build the PV generation system. According to the voltage and power requirements, we customized the series and parallel combination of the solar cells and modules. To make sure the modules output maximum power, the maximum power point tracking (MPPT) controller is modeled with the algorithm

to track the maximum power by directly perturbing the output voltage of the PV array [48,49].

### **3.4.2 ESS**

An in-built library model of the battery based on the Shepherd model in MATLAB-Simulink was used to simulate the ESS.

### **3.4.3 Load simulation**

Loads in 375 V power buses and the 750 V power bus were modeled with resistances, and the constant power load in the 48 V power bus was modeled with constant current source and resistance. Different load level analyses were carried out when conducting the DC converter controller analysis by adjusting the load level by percentage.

## **4. Simulation results**

### **4.1 MATLAB-Simulink model configuration**

The model was built based on the methodology described in Section 3. Figure 4 illustrates the configuration of the microgrid.

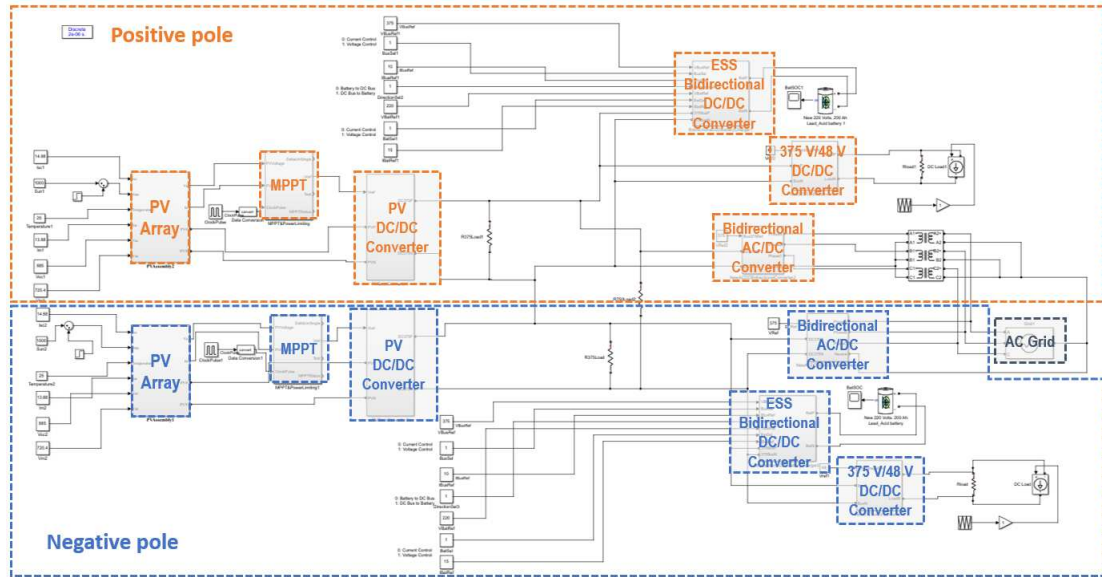


**Figure 4. Simulink model of the demonstration building's DC microgrids**

## 4.2 Design specifications of converters in simulation

The 375 V power bus on each pole has four converters. This includes a bidirectional AC/DC converter connecting the DC power bus to the grid, a DC/DC buck converter connecting the PV array to the 375 V power bus, a DC/DC buck converter connecting a 48 V power bus to a 375 V power bus, and a DC/DC bidirectional converter connecting the ESS to a 375 V power bus. The design of these converters was carried out based on methods introduced in Section 3.3.

### 4.2.1 Grid-tied AC/DC converter

The AC/DC converters are 20 kW, two-quadrant PWM converters, to which PI control is applied. Two bidirectional AC/DC converters connect the grid and the positive/negative wire in the grid-connected mode, respectively. These converters manage to maintain a balance

between loads and power supplies, transferring power either from the AC grid to the DC microgrid or from the DC microgrid to the AC grid. They control the bus voltage in either circumstance. The power flow direction of the AC/DC controller can be adjusted automatically by the regulator in its control loop. In the control loop, there is an outer voltage loop and an inner current loop. The outer voltage loop controls the 375 V bus voltage, while the inner current loop regulates the waveforms of the current in the AC side so that it can achieve plus- or minus-one power factor. In the plus-one power factor condition, the phase of the voltage generated by the converter bridge lags the phase of the voltage of the AC grid, while in the minus-one power factor condition, it leads to that of the AC grid. The bidirectional power flow between the AC side and DC side is made possible by the characteristic of active power flowing from the voltage with a leading phase to the voltage with the lagging phase.

#### **4.2.2 PV array DC/DC buck converter**

A DC/DC buck converter is used to connect the PV generation to the power bus. The PV array is the input port, and a DC 375 V bus is the output of this converter. There were two sets of PV arrays—MPPT controllers and DC/DC converters—symmetrically connected to a positive DC 375 V bus and a negative DC 375 V bus, respectively.

In the converter, the main circuit filter inductor of the converter is 6 millihenries (mH). The capacitors at the input port (two capacitors of 4,700  $\mu\text{F}$  in parallel) and output port (six capacitors of 470  $\mu\text{F}$  in parallel) measure 9,400 microfarads ( $\mu\text{F}$ ) and 2,820  $\mu\text{F}$ , respectively.

Through adjustment, the switching frequency is 5 kilohertz (kHz) and the 0 decibel (dB)

crossing frequency of the whole loop is one-fifth of the switching frequency. The gain and phase margins of the loop are 9.8 dB and 55° at rating power.

#### **4.2.3 375 V to 48 V DC/DC buck converter**

This DC/DC converter that connects 375 V DC bus and 48 V DC bus is a peak current mode controlled buck converter with a rating power of 500 W. The main circuit filter inductor is 3.5 mH, and the capacitor measures 2,820  $\mu$ F, which is made by six capacitors of 470 F in parallel. The converter has a switching frequency of 5 kHz, while the 0 dB crossing frequency of the opened control and power loop at rating power is one-tenth of the switching frequency. The gain margin and phase margin of the converter at the rating power measure 12.6 dB and 64.1°, respectively.

#### **4.2.4 ESS bidirectional DC/DC buck and boost converter**

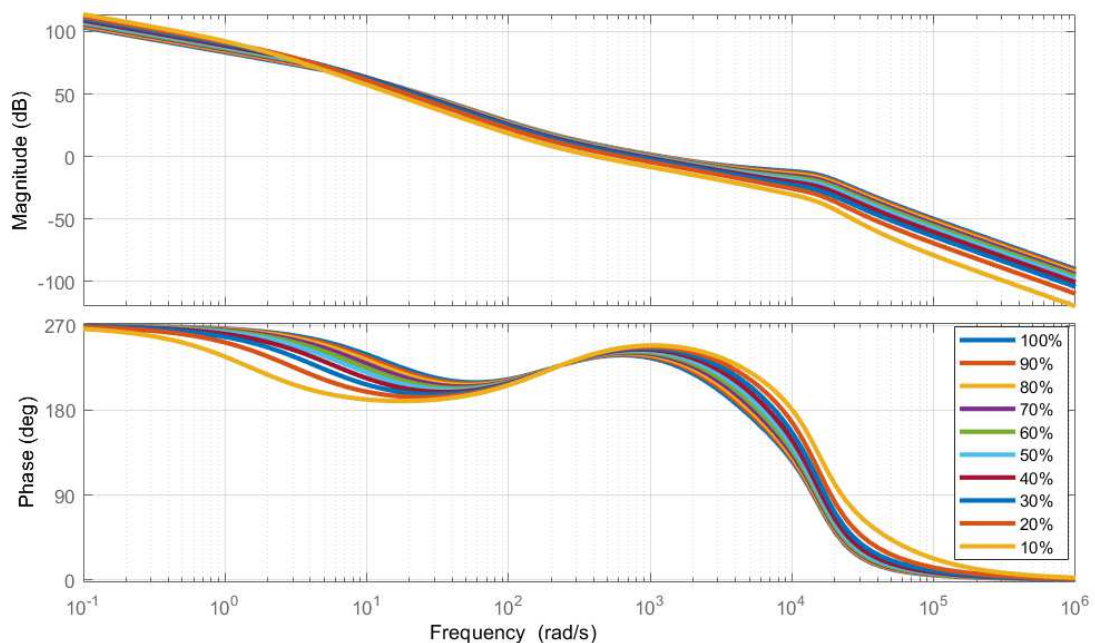
A bidirectional DC/DC converter was built to charge and discharge the battery according to scenarios. The bidirectional converter is configured as a buck or a boost, which has four different operation modes: (a) bus voltage control, (b) power output, (c) constant current charging, and (d) constant voltage charging. The first, the bus voltage control mode, is used in the off-grid mode when the system operates off-grid. The other three modes are used in grid-connected mode, in discharging or charging scenarios with different control strategies.

In the off-grid mode, the bus voltage of the DC microgrid is controlled by the bidirectional DC/DC converter, which can balance the power supply by changing the direction of the power flow. Two insulated gate bipolar transistors (IGBTs) inside the converter form a bridge

leg so that it can work in either direction. In case of more power than load in the DC microgrid, the power transfers from DC microgrids to the battery storage system.

When the converter works in grid-connected scenarios, mode b uses a battery storage system to provide all or part of the power required. The building load can be provided by PV generation, battery storage, and grid, depending on different control strategies and ESS management. Modes c and d are two different charging modes that are dependent on a different state of the battery, the supply and demand of the grid, and other situations.

Different load level analysis was carried out when conducting the DC/DC converter controller analysis by adjusting the load level from 10% of the rated power to 100%, as marked in Figure 5. By conducting the Bode analysis presented in Figure 5a, we were able to see the change of gain margin and phase margin when the load levels increase. In full load, the gain margin and phase margin at the rating power measured 8.7 dB and 52.5°, respectively. Similarly, Figure 5b depicts the step response under different loads.



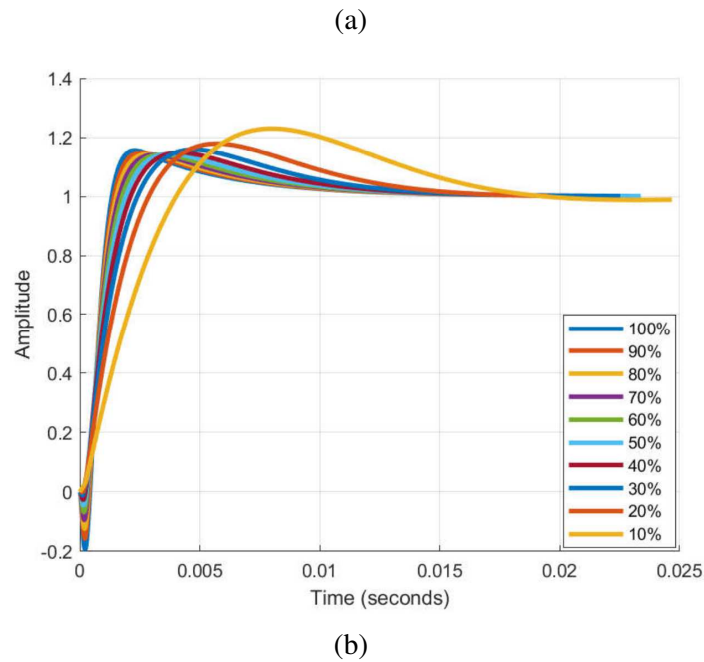


**Figure 5. (a) Bode analysis, and (b) step analysis of boost mode bidirectional DC/DC converter at different load levels**

### 4.3 Scenario setting

Because DC lacks the reactive part of the impedance, many phenomena can be more detrimental in DC networks than in AC ones [5]. To further verify the operational performance of the design and modeling of the DC microgrids in this office building under various source and load conditions, different scenarios of the model were simulated. A dynamic simulation of scenarios was made in a MATLAB-Simulink environment to verify the power dynamic characteristics. Both grid-connected and off-grid modes were taken into consideration, and different impact sources, including fluctuations from distributed generation (DG) resources, load, and grid side were considered. The tested scenarios are listed below in Table 1.

The research considered a few interrupted events (events **a** to **e**) in its modeling analysis. Event **a** represented the impacts of fluctuations from DG in the off-grid mode, where two cases—PV output power fluctuation and PV source disconnection—were considered. Event **b** verified the impact of load fluctuation happening in DC buses of different voltage levels—750 V, 375 V, and 48 V DC bus—in the off-grid mode. The rest of the events considered the grid-connected mode with similar settings. Events **c** and **d** covered DGs and load fluctuations, respectively, in grid-connected mode. Event **e** took into account the connection to the utility grid, including voltage fluctuation from the AC side, grid disconnection, and grid reconnection. Event **f** tried to verify system stability when unbalance occurred in the positive and negative power, covering unbalanced load and unbalanced DGs fluctuation. Given that the system is more stable with the regulation of the grid in grid-connected and off-grid mode scenarios with the same impact sources, only the scenarios in off-grid mode are discussed.

The average PV power output during the 0.3 second (s) time section was 10.44 kW. The ESS uses a lead-acid battery pack with a nominal voltage of 220 V, a capacity of 200 amp hours, and an initial state-of-charge of 99.5% to store energy. The transient loads on the 48 V, 375 V, and 750 V power buses were modeled through constant resistances, and the rated power on these power buses was, respectively, 0.25 kW, 7.03 kW (each pole), and 14.06 kW.

***Table 1. Different modes and scenarios of the simulation***

<b>Mode</b>	<b>Impact source</b>	<b>Scenarios</b>
Off-grid	<b>a:</b> Distributed generation (DG)	<b>a.1</b> PV output power fluctuation

		<b>a.2</b> PV sources shut down
	<b>b:</b> Load fluctuation	<b>b.1</b> 750 V DC bus shut down <b>b.2</b> 375 V DC bus shut down <b>b.3</b> 48 V DC bus shut down
Grid-connected	<b>c:</b> DG	<b>c.1</b> PV output power fluctuation <b>c.2</b> PV sources shut down
	<b>d:</b> Load fluctuation	<b>d.1</b> 750 V DC bus shut down <b>d.2</b> +375 V DC bus shut down <b>d.3</b> 48 V DC bus shut down
	<b>e:</b> Connection to the utility grid	<b>e.1</b> Utility grid AC side voltage fluctuation <b>e.2</b> Grid disconnection <b>e.3</b> Grid reconnection
Off-grid / Grid-connected	<b>f:</b> Unbalanced load / unbalanced DG fluctuation	<b>f.1</b> Single-pole off-grid, PV fluctuation simulation <b>f.2</b> DG fluctuation and load fluctuation in single-pole, grid-connected mode <b>f.3</b> Other cases mentioned above

Although variable events were tested, only the most representative ones are presented in Sections 4.4 to 4.6. In grid-connected mode, the voltage buses were regulated by the AC grid; and in off-grid mode, the voltage buses were regulated by the ESS that discharged to the supply power. As the power regulation ability of the latter is weaker, in events **a**, **b**, **c**, and **d**, only **a** and **b** are covered in Section 4.4. Section 4.5 presents the testing results of Event **e**. Section 4.6 takes into account system stability when unbalance happened in each pole.

#### 4.4 Microgrid performance with loads and PV fluctuations (Event a and Event b)

The building-scale DC microgrid systems can be complicated due to faults in different situations. This section describes the tests conducted to evaluate the power quality provided and to verify the stability, robustness, and safety of the system when fluctuations from load or

PV generation occur. These situations were verified in the islanded mode, considering that without the regulation of the grid, maintaining system stability is harder. In the simulated scenarios, voltage/current control, and different power flow directions did not exert great influence on system performance. The results were obtained when the voltage control was used on the power bus and the current control was used on the ESS. The power flow direction was voltage bus to ESS.

#### 4.4.1 Fluctuation of DGs

Figure 6 shows the voltage responses of the voltage bus bars in a scenario where the PV generation output falls to zero at 0.10 s and recovers to twice the original power at 0.18s. As the fluctuation was symmetrical in both poles the voltage level of power Bus 1 and power Bus 2 coincided.

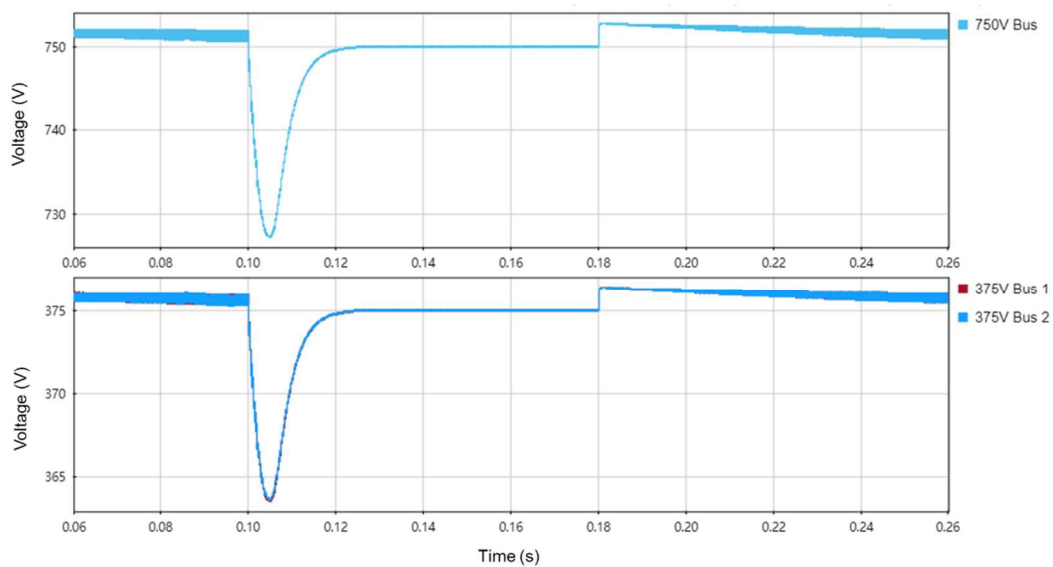


**Figure 6. The voltage response of PV fluctuation (a.2)**

The 750 V power bus dropped by 4.06% when the PV generation shut down, which is higher

than 0.79% in the case of the same fluctuation in grid-connected mode. The reason for this phenomenon is that, unlike in the grid-connected mode, when the system was off-grid the ESS took more responsibility for stabilizing bus voltage. In contrast, in grid-connected mode, most of the fluctuation was reduced and most of the stabilizing capability relied on the AC power grid.

#### 4.4.2 Load fluctuation

The impact of load fluctuation was studied by testing the load switching off and on in 750 V, +/-375 V, and 48 V bus bar. The simulation setup in this scenario was identical with the load fluctuation studies in grid-connected mode; the load disconnected at 0.10 s and connected back again at 0.20 s. In response to the load fluctuation, the power bus voltage also fluctuated. Figures 7–9 illustrate the voltage fluctuation level in each power level when sudden disconnection of loads happened in different locations.

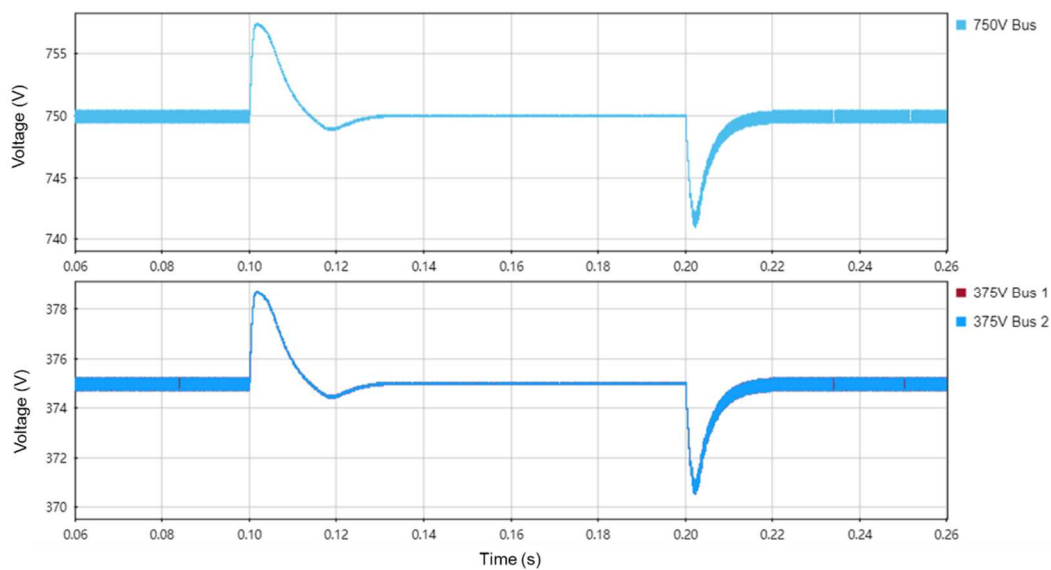


**Figure 7. The voltage response of 750 V load fluctuation (b.1)**

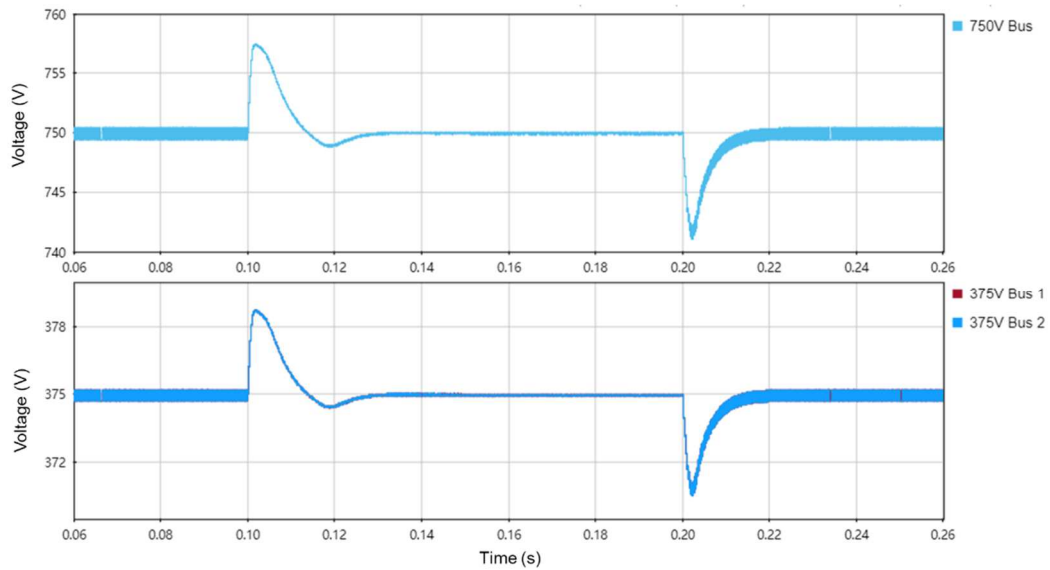


**Figure 8. The voltage response of 375 V load fluctuation (b.2)**

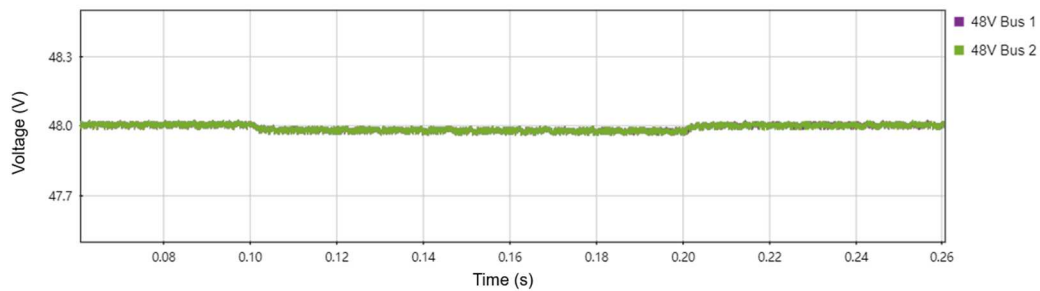


**Figure 9. The voltage response of 48 V load fluctuation (b.3)**

When load disconnection happened in the 750 V voltage level or the 375 V level, the greatest swell and sag were, respectively, 0.99% and 1.12% to the nominal voltage of 750 V and  $\pm 375$  V, while the 48 V power bus was unaffected. When the load disconnection happened at the 48 V level, the greatest swell and sag were, respectively, 0.068% and 0.085% to the nominal voltage of 750 V and  $\pm 375$  V.

#### **4.5 Microgrid performance with grid side voltage fluctuation (Event e)**

As mentioned, in grid-connected mode, the power buses are regulated by both of the power sources, the grid, and the ESS, which stabilizes the voltage level and increases its robustness compared to operation in the off-grid mode. The grid-connected transient simulation showed satisfying stability in the last two sections with the support and regulation of the AC grid. For brevity, this section will not include the DG and load fluctuation scenarios, which were introduced in the off-grid mode. Nevertheless, it should be considered to what extent stability can be maintained when the grid side voltage fluctuates.

This scenario intended to simulate the real possible faults in the application. It was our purpose to investigate how the system would react to a sudden drop or even a shutdown of the grid side. We assumed that when a grid side voltage fluctuation occurs, it takes 0.02 seconds for the system to react—0.02 seconds of voltage drop before the ESS's activation to stabilize the power level of the main power bus.

#### **4.5.1 Partial voltage drops**

Figure 10 shows the result of the scenario where grid voltage drops 50% from its normal operation mode at 0.10 s and recovers at 0.2 s. The 750 V voltage bus and 375 V voltage bus quickly respond to such a fluctuation, and the voltage is under control within 0.04s. In a real-life application, we can predict such a severe fluctuation of city grid voltage is unlikely to happen in most cases. The stability and robustness of grid voltage deserve more consideration, and safety measures and emergency solutions shall be utilized to avoid deep fluctuation.

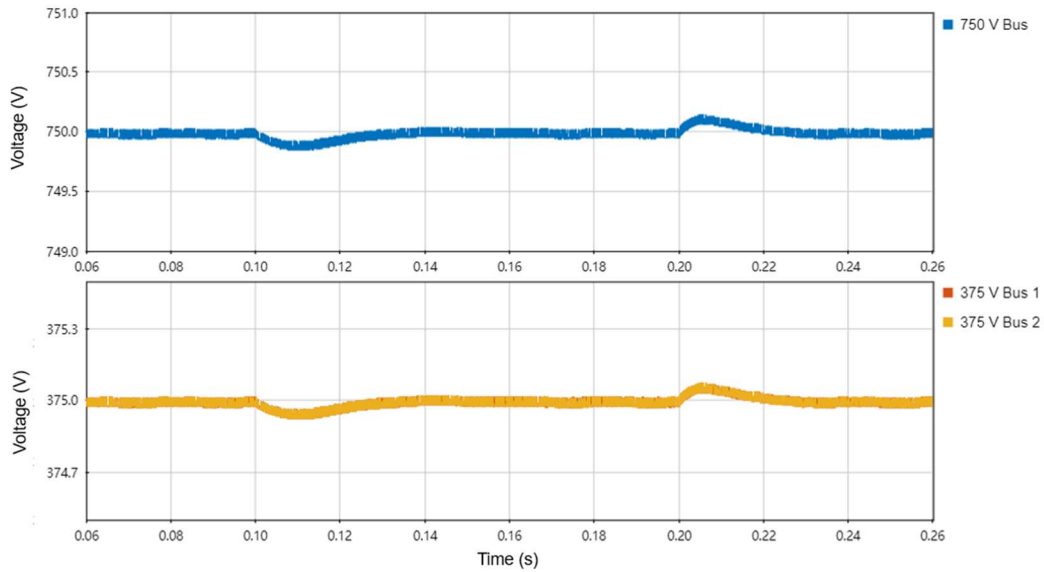


**Figure 10. The voltage response of 50% grid voltage drop (e.1)**

#### **4.5.2 Disconnection from the grid**

Figure 11 illustrates how the system responds to a sudden disconnection from the grid. The incident happened at 0.10 s, and the bidirectional DC/DC converter connected to the ESS, taking 20 milliseconds (ms) to react and switch the system into a voltage-controlled mode supplied and regulated by two batteries providing storage at both poles. Thus, after 20 ms of linear voltage drop in the 750 V and 375 V power buses, the system was back in balance. The greatest sag during this incident was 0.83% of the nominal voltage, happening at 0.12 s. The peak voltage happened at 0.123 s with a 0.51% swell above the nominal voltage.

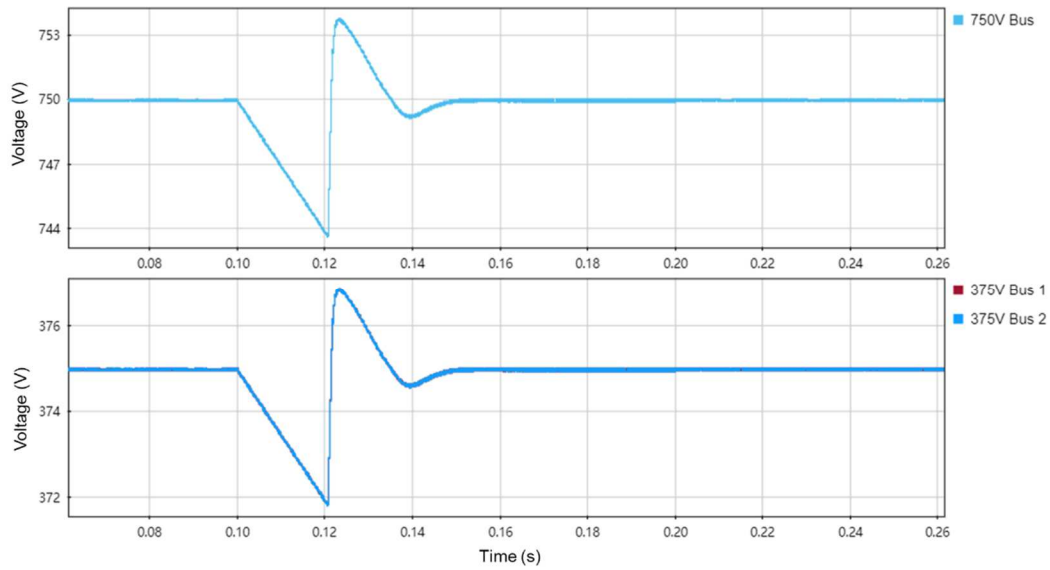


**Figure 11. The voltage response of grid disconnection (e.2)**

#### 4.5.3 Grid reconnection

This scenario simulated the transition from off-grid to grid-connected mode. In off-grid mode, the system is either powered by the ESS with the battery set discharging energy or by PV while the ESS converter controls the DC bus to charge the battery. It is also likely that both PV and ESS are supplying the microgrid. The grid reconnection happened at 0.10 s, after which the ESS bidirectional DC/DC converter switched from battery discharging to battery charging mode at 0.12 s. The oscillation range shrunk at 0.10 s as a response to the grid reconnection which further regulates the voltage. A mild dip happened at 0.12 s when the bidirectional DC/DC converter switched directions. The system stayed stable during the reconnection process as shown in Figure 12.

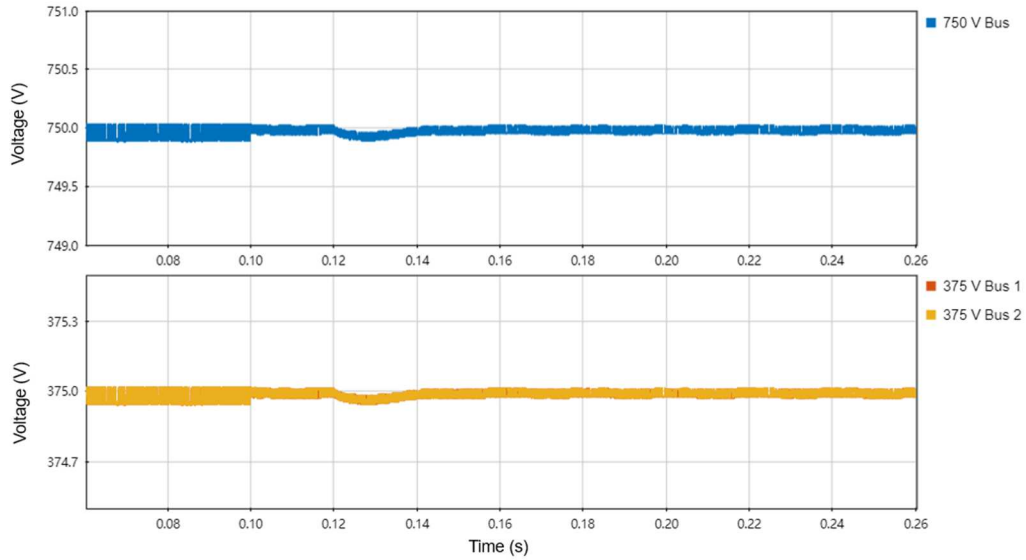


**Figure 12. The voltage response of grid reconnection (e.3)**

#### **4.6 Microgrid performance in unbalanced load/DGs fluctuation (Event f)**

Voltage balancing in both poles is an important issue in bipolar DC buildings. A rich literature has provided a variety of methods to balance the voltage level in each pole with unbalanced sources, loads, and faults. The voltage balancing capability was also tested in the proposed loose-coupled bipolar system to study the system response to unbalanced fluctuation or modes of connection in each pole. The results show the stability and robustness of the system in these scenarios.

##### **4.6.1 Single-pole, off-grid, PV fluctuation simulation**

This scenario tested the power response of PV array fluctuation with one of the 375 V power buses connected to the grid and the other off-grid. When PV output disconnection happens, the unbalancing of the poles happens due to their different abilities to regulate power grid voltage. The resulting maximum voltage sag in the 750 V power bus was 2% at 0.105 s as

shown in Figure 13. The test also found that the grid-connected mode and off-grid mode showed a difference in the maximum loads they can support. The off-grid mode would have a voltage drop if the loads on the 375 V bus or 750 V bus appeared to be higher than the battery power limit for the battery power output.

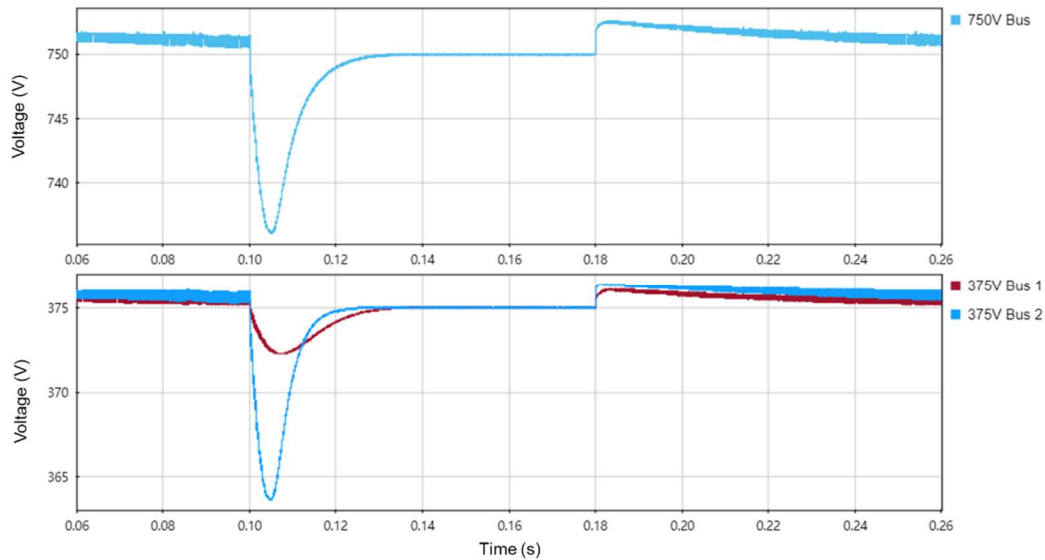


**Figure 13. The voltage response of PV fluctuation with different grid connecting mode**

(f.1)

#### 4.6.2 DG fluctuation and load fluctuation in single-pole, grid-connected mode

This scenario simulated the impact of unbalanced fluctuations on each pole, with the goal of verifying that the loose-coupled bipolar system can maintain one pole unimpacted from the other pole, while the latter fluctuates. In this case, DG fluctuations and load fluctuations happened in one power bus (375 V Bus 1), while the other power bus remained stable. In 375 V Bus 1, the PV array output fell to zero at 0.10 s and recovered to twice the original power at 0.18 s. In addition, the loads in the 375 V power bus were disconnected at 0.10 s and

recovered at 0.20 s. The 375 V Bus 1 maintained its stability, and the 375 V Bus 2 was unaffected. Overall, the resulting voltage response was satisfying, as shown in Figure 14.

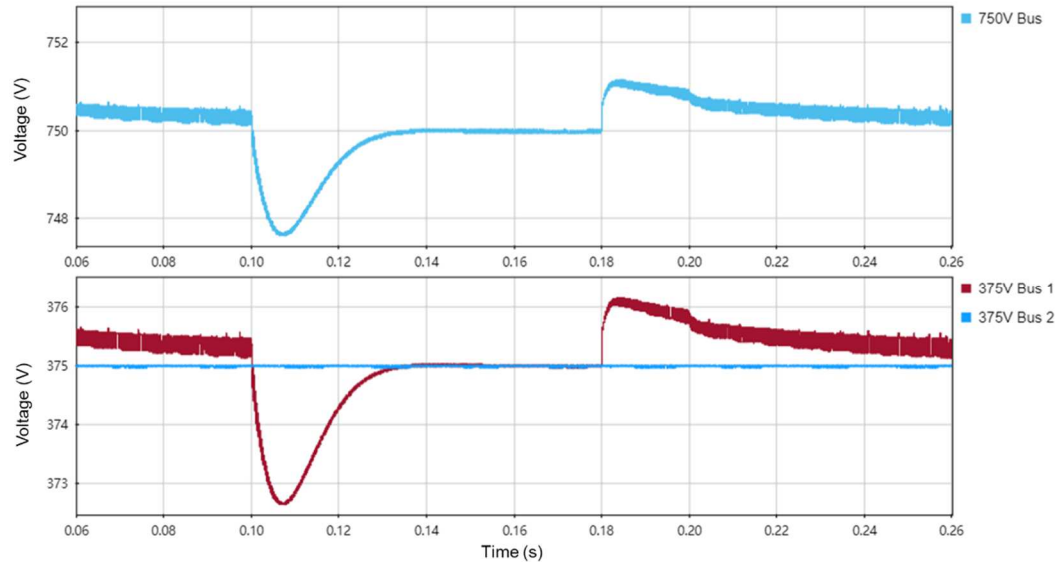


**Figure 14. The voltage response of DG fluctuation and load fluctuation in one pole (f.2)**

#### 4.7 Analysis of potential causes for instability

As introduced in the Methodology chapter, we utilized zero-pole placement to design the controller parameters. In the simulation, the system performed well under various disruptive scenarios, which demonstrates good system stability theoretically. However, in practice, the potential instability of the system may happen due to internal or external causes. Digital simulation assumes perfect knowledge of system circumstances and ideal configuration settings exactly as designed. Nevertheless, in reality, many settings may lead to instability if improperly configured. Two possible sources that may cause instability of the system were considered in this chapter to further verify the system stability robustness.

The bidirectional converter connecting the battery and the 375V power grid was used as the

representative for analysis in this chapter.

### 4.7.1 Controller zero-pole shift

One potential cause of instability is zero-pole shift due to the error of the resistance and capacitance in the analog control circuit. In the simulation, we used digital implementation of components with precise parameters. We considered 5% of zero-pole shift due to the error of component parameters in practice. Figure 15 presents the Bode diagram and step response of the 5% controller zero-pole shift.

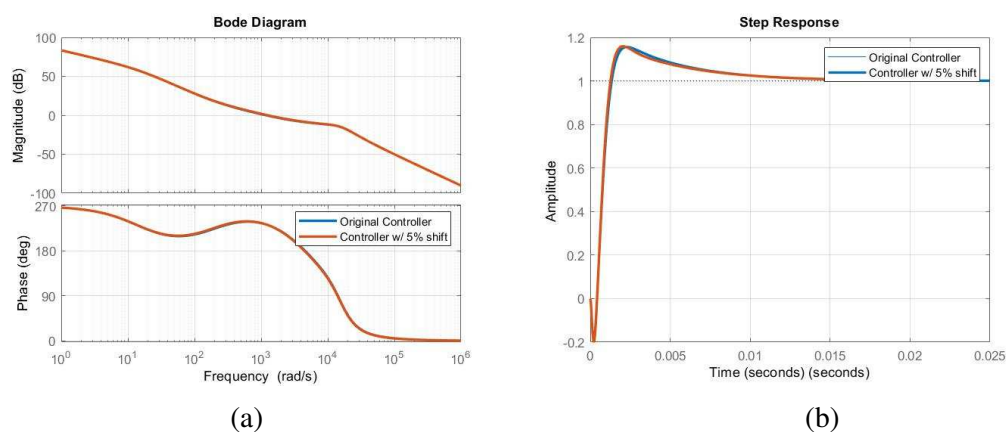


**Figure 15. (a) Bode analysis, and (b) step analysis of a controller zero-pole shift of 5%**

With the original controller parameter, the gain margin was 8.8 dB and 52.7 degrees. With a 5% of the zero-pole shift to the right, the gain margin and the phase margin changed to 8.4 dB and 51.7 degrees. No significant impact was observed in either the frequency or time domains.

### 4.7.2 Robustness analysis on component error

Instability of the system also may be caused by an error in external parameters. Ignoring

minor parameters in simulation or incorrect setting of modeling parameters can lead to system instability. To further verify the robustness of the system, we considered errors introduced by component parameter errors. We analyzed the impact of differences between the actual values and the nominal values of inductances and capacitances.

We assumed the actual inductance varies between 90% to 110% of the nominal value and that the actual capacitance varies within the range of 80% to 120% of the nominal value. The controller parameter was designed based on the nominal value of the capacitor and inductor. Considering an interval of 1%, we used the Bode diagram to analyze the controller performance.

Figure 16 shows that the impact of error introduced by the inductor and capacitor is relatively small and would not affect the system stability.

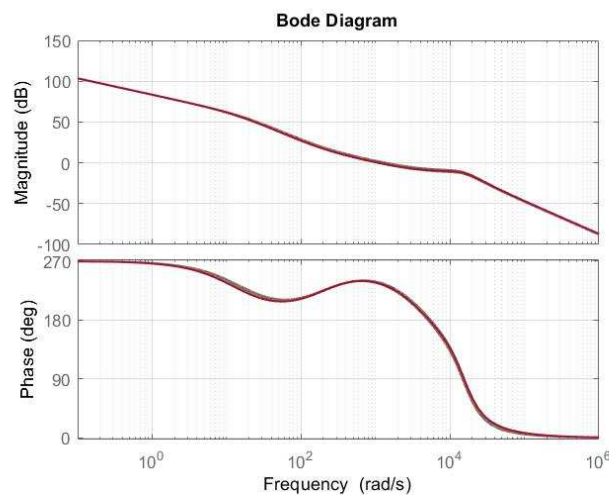


**Figure 16. Bode analysis of error introduced by the inductor and capacitor**

#### **4.7.3 Robustness analysis on noises**

In practice, noise can happen in different places of the system circuit, such as noise at the high-frequency switching and noise at a voltage or current measurement. We added band-limited white noise to simulate voltage measurement noise in the ESS bidirectional DC/DC buck and boost converter discharging controller feedback loop. The white noise block was only added on only one of the poles. The positive voltage bus with noise and the negative voltage bus without noise provided a comparison for us to better understand the impact of noise in the system.

As shown in Figure 17, the noise magnitude was about  $\pm 44$  V, which is about 12% of the voltage of the 375 V voltage bus. The noise frequency was set to be 8 MHz. The correlation time was smaller than the shortest time constant of the system.

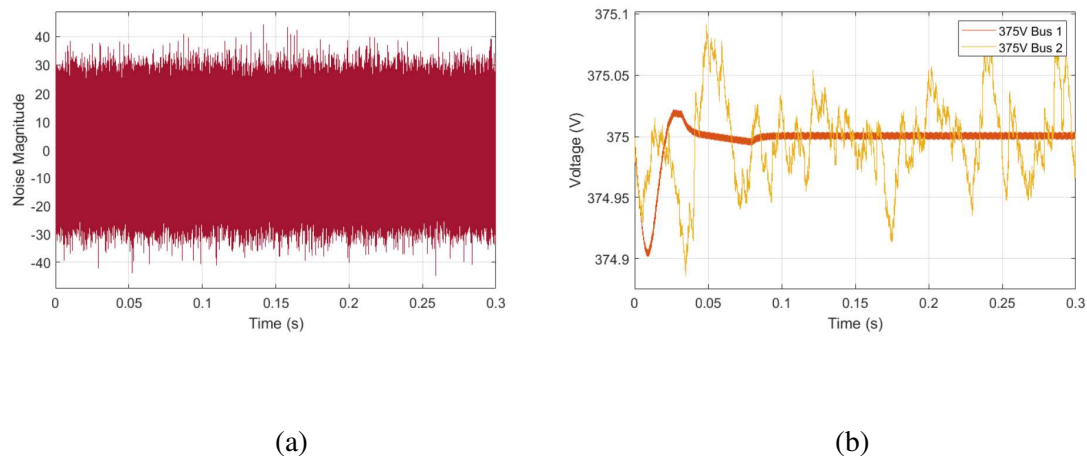


**Figure 17. Analysis of voltage measurement noise in the ESS bidirectional DC/DC buck and boost converter. (a) noise magnitude; (b) voltage output of the 375 V buses**

Figure 17b shows that adding noise had some small impact on 375 V Bus 1 voltage fluctuation. However, the voltage fluctuation was very small (less than  $\pm 1\%$ ) and would not

affect system stability. The simulation model proves that power electronics and control design in the case DC microgrid system can successfully handle typical noise without causing an impact on system stability.

#### **4.7.4 Limitations and other potential issues**

Besides the potential causes of instability verified, the system also has limitations and other potential issues that may arise during operation.

As the input signals during simulation are ideal, signal filters were not modeled in this simulation model. However, in actual cases, a filter process is often observed to eliminate system noise, which may also introduce phase lagging into the control loop. Besides signal filtering issues, in the distribution system, faults and errors may happen in various forms. Here we only discuss some of the most representative scenarios to verify the system robustness. In reality, sometimes more advanced fault detection and diagnosis methods are often required to comprehensively analyze faults.

### **5. Conclusion**

This project studied the design and simulation of a DC building with a loose-coupled bipolar system. Topics related to the characteristics of DC microgrids and their components are reviewed in detail. We developed a novel concept of loose-coupled bipolar DC power system topology in buildings. To test the system performance, a generic DC power quality simulation framework was established. A few power quality disruptive scenarios were developed and were used to model a real-world office building DC power system using the loose-coupled

bipolar system. In addition, the bipolar DC power system's dynamic performance was validated through simulation.

Multiple operating scenarios of DC power system disruption were generated to analyze the impact of DG fluctuation, load fluctuation, and grid shutdown in both grid-connected mode and off-grid mode. The result of simulation analysis showed that this design of DC microgrids and its control system with a loose-coupled bipolar  $\pm 375$  V DC bus bar, 48 V end devices, PV generation, and ESS can maintain its stability in multiple operational situations and adverse events. It was found that, in grid-connected mode, the grid makes a great contribution to keeping the system stable, while in off-grid mode, the battery storage system will support power bus bars to maintain stability.

Overall, the research showed plausible results of the stability and robustness of the DC power system. Simulation work has demonstrated that the loose-coupled bipolar DC power system, with proper controller design, can achieve good robustness when a disruptive event occurs. The bus line power voltage can be controlled within a very short period of time when the disruptive event happens. Because of its loosely coupled nature, the bipolar DC system also can successfully isolate disruptive events propagated from one pole to another pole or from a 375 V circuit to a 48 V or 24 V circuit. This new DC power architecture has greatly improved the system stability compared with an AC or a single polar power DC building power system. Therefore, this study presents a successful building-scale design and simulation of a loose-coupled bipolar DC microgrid construction, integrated with many components, and provides an extensive analysis of information and characteristics regarding the model.

## **CRedit authorship contribution statement**

**Ruiting Wang:** Overall modeling, Data compilation, Writing. **Wei Feng:** Conceptualization, Project management, Abstract, introduction, conclusion section writing. **Huijie Xue:** Model development; **Daniel Gerber:** Model development, Testing. **Yutong Li:** Bi-polar structure development, Result validation. **Hao bin:** Bi-polar structure development, Result check. **Yibo Wang:** Literature, Result check.

## **Declaration of Competing Interest**

The authors declare that they have no known competing financial interests or personal relationships that could have appeared to influence the work reported in this paper.

## **Acknowledgements**

The U.S. authors recognize Lawrence Berkeley National Laboratory's support from the U.S. Department of Energy under Contract No. DEAC02-05CH11231. The research project is also supported by the High Efficiency Integration of Multiple Renewable Energy Technologies: International Research (Project Number: GJTD2018-05), Chinese Academy of Sciences; City Energy Efficiency and Low Carbon Solution Tool Research and Development, Chinese Ministry of Science and Technology (Project Number:2017YFE0105600); Sino-US Low Carbon City Demonstration, Shenzhen Institute of Building Research (Project Number: JK-WLDT-038).

The U.S. Government retains a non-exclusive, paid-up, irrevocable, world-wide license to

publish or reproduce the published form of this manuscript, or allow others to do so, for U.S.

Government purposes.

## References

- [1] Vossos V, Johnson K, Kloss M, Khattar M, Gerber D, Brown R. Lawrence Berkeley National Laboratory Review of DC Power Distribution in Buildings : A Technology and Market Assessment 2017.
- [2] Starke M, Member S, Tolbert LM, Member S. AC vs . DC Distribution : A Loss Comparison 2008.
- [3] Porter SF, Denkenberger D, Mercier C, May-ostendorp P, Consulting X. Reviving the War of Currents : Opportunities to Save Energy with DC Distribution in Commercial Buildings 2014:85–97.
- [4] Marnay C, Chatzivasileiadis S, Abbey C, Iravani R, Joos G, Lombardi P, et al. Microgrid evolution roadmap. Proc - 2015 Int Symp Smart Electr Distrib Syst Technol EDST 2015 2015:139–44. <https://doi.org/10.1109/SEDST.2015.7315197>.
- [5] Barros J, Apráiz M de, Diego RI. Power Quality in DC Distribution Networks. Energies 2019;12:848–60. <https://doi.org/10.3390/en12050848>.
- [6] Rawat GS, Sathans. Survey on DC microgrid architecture, power quality issues and control strategies. Proc 2nd Int Conf Inven Syst Control ICISC 2018 2018:500–5. <https://doi.org/10.1109/ICISC.2018.8399123>.
- [7] Berry FC. Modeling of DC spacecraft power systems 1995.
- [8] Grassi F, Pignari SA, Wolf J. Channel characterization and EMC assessment of a PLC system for spacecraft DC differential power buses. IEEE Trans Electromagn Compat 2011;53:664–75. <https://doi.org/10.1109/TEMC.2011.2125967>.
- [9] Kintner D. Duke Energy - EPRI DC Powered Data Center Demonstration: Executive Summary. Energy 2011.
- [10] Thompson DJ. DC voltage stabilization control in telecommunications DC distribution systems. INTELEC, Int Telecommun Energy Conf 2002:74–8.
- [11] Wang F, Lei Z, Xu X, Shu X. Topology deduction and analysis of voltage balancers for DC microgrid. IEEE J Emerg Sel Top Power Electron 2017;5:672–80. <https://doi.org/10.1109/JESTPE.2016.2638959>.
- [12] Chew BSH, Xu Y, Wu Q. Voltage Balancing for Bipolar DC Distribution Grids: A Power Flow Based Binary Integer Multi-Objective Optimization Approach. IEEE Trans Power Syst 2019;34:28–39. <https://doi.org/10.1109/TPWRS.2018.2866817>.
- [13] Boeke U, Wendt M. DC power grids for buildings. 2015 IEEE 1st Int Conf Direct Curr Microgrids, ICDCM 2015 2015:210–4. <https://doi.org/10.1109/ICDCM.2015.7152040>.
- [14] Fregosi D, Ravula S, Brhlik D, Saussele J, Frank S, Bonnema E, et al. A comparative study of DC and AC microgrids in commercial buildings across different climates and operating profiles. 2015 IEEE 1st Int Conf Direct Curr Microgrids, ICDCM 2015 2015:159–64. <https://doi.org/10.1109/ICDCM.2015.7152031>.

- [15] Weiss R, Ott L, Boeke U. Energy efficient low-voltage DC-grids for commercial buildings. 2015 IEEE 1st Int Conf Direct Curr Microgrids, ICDCM 2015 2015:154–8. <https://doi.org/10.1109/ICDCM.2015.7152030>.
- [16] Gerber DL, Vossos V, Feng W, Marnay C, Nordman B, Brown R. A simulation-based efficiency comparison of AC and DC power distribution networks in commercial buildings. *Appl Energy* 2018;210:1167–87. <https://doi.org/10.1016/j.apenergy.2017.05.179>.
- [17] Vossos V, Garbesi K, Shen H. Energy savings from direct-DC in U . S . residential buildings. *Energy Build* 2014;68:223–31. <https://doi.org/10.1016/j.enbuild.2013.09.009>.
- [18] Savage, Paul, Nordhaus, Robert R., Jamieson SP. From silos to systems: issues in clean energy and climate change: DC microgrids: benefits and barriers. Tech Rep Yale Sch For Environ Sci 2010.
- [19] Backhaus S, Swift GW. DOE DC microgrid scoping study-opportunities and challenges. 2015 IEEE 1st Int Conf Direct Curr Microgrids, ICDCM 2015 2015:43–4. <https://doi.org/10.1109/ICDCM.2015.7152007>.
- [20] Broeck G Van Den, Stuyts J, Driesen J. A critical review of power quality standards and definitions applied to DC microgrids. *Appl Energy* 2018;229:281–8. <https://doi.org/10.1016/j.apenergy.2018.07.058>.
- [21] Nilsson D, Sannino A. Efficiency analysis of low- and medium-voltage dc distribution systems. 2004 IEEE Power Eng Soc Gen Meet 2004;2:2315–21. <https://doi.org/10.1109/PES.2004.1373299>.
- [22] Mahdavyfakhr M, Rashidirad N, Hamzeh M, Sheshyekani K, Afjei E. Stability improvement of DC grids involving a large number of parallel solar power optimizers: An active damping approach. *Appl Energy* 2017;203:364–72. <https://doi.org/10.1016/j.apenergy.2017.06.044>.
- [23] Emadi A, Khaligh A, Rivetta CH, Williamson GA. Constant power loads and negative impedance instability in automotive systems: Definition, modeling, stability, and control of power electronic converters and motor drives. *IEEE Trans Veh Technol* 2006;55:1112–25. <https://doi.org/10.1109/TVT.2006.877483>.
- [24] García O, Zumel P, de Castro A, Cobos JA. Automotive dc-dc bidirectional converter made with many interleaved buck stages. *IEEE Trans Power Electron* 2006;21:578–86. <https://doi.org/10.1109/TPEL.2006.872379>.
- [25] Kakigano H, Miura Y, Ise T. Low-voltage bipolar-type dc microgrid for super high quality distribution. *IEEE Trans Power Electron* 2010;25:3066–75. <https://doi.org/10.1109/TPEL.2010.2077682>.
- [26] Kakigano H, Miura Y, Ise T, Uchida R. DC micro-grid for super high quality distribution - system configuration and control of distributed generations and energy storage devices. 2006 37th IEEE Power Electron Spec Conf 2006:1–7. <https://doi.org/10.1109/PESC.2006.1712250>.
- [27] Momose T, Hayakawa H, Fujimoto H, Kakigano H, Miura Y, Ise T. Fundamental Characteristics of DC Microgrid for Residential Houses with Cogeneration System in Each House. 2008 IEEE Power Energy Soc Gen Meet - Convers Deliv Electr Energy 21st Century 2008:1–8. <https://doi.org/10.1109/PES.2008.4596210>.

- [28] Van Den Broeck G, De Breucker S, Beerten J, Zwysen J, Dalla Vecchia M, Driesen J. Analysis of three-level converters with voltage balancing capability in bipolar DC distribution networks. 2017 IEEE 2nd Int Conf Direct Curr Microgrids, ICDCM 2017 2017;248–55. <https://doi.org/10.1109/ICDCM.2017.8001052>.
- [29] Lago J, Heldwein ML. Operation and control-oriented modeling of a power converter for current balancing and stability improvement of DC active distribution networks. IEEE Trans Power Electron 2011;26:877–85. <https://doi.org/10.1109/TPEL.2011.2105284>.
- [30] Liao J, Zhou N, Huang Y, Wang Q. Unbalanced Voltage Suppression in a Bipolar DC Distribution Network Based on DC Electric Springs. IEEE Trans Smart Grid 2019;PP:1. <https://doi.org/10.1109/TSG.2019.2941874>.
- [31] Middlebrook RD. Topics in Multiple-Loop Regulators and Current- Mode Programming. IEEE Trans Power Electron 1987;109–24.
- [32] Loh PC, Holmes DG. Analysis of multiloop control strategies for LC/CL/LCL-filtered voltage-source and current-source inverters. IEEE Trans Ind Appl 2005;41:644–54. <https://doi.org/10.1109/TIA.2005.844860>.
- [33] Blaabjerg F, Teodorescu R, Liserre M, Timbus A V. Overview of control and grid synchronization for distributed power generation systems. IEEE Trans Ind Electron 2006;53:1398–409. <https://doi.org/10.1109/TIE.2006.881997>.
- [34] Teodorescu R, Blaabjerg F, Liserre M, Loh PC. Proportional-resonant controllers and filters for grid-connected. IEE Proceedings-Electric Power Appl 2006;153:750–62. <https://doi.org/10.1049/ip-epa:20060008>.
- [35] Tai TL, Chen JS. UPS inverter design using discrete-time sliding-mode control scheme. IEEE Trans Ind Electron 2002;49:67–75. <https://doi.org/10.1109/41.982250>.
- [36] Kim DE, Lee DC. Feedback linearization control of three-phase UPS inverter systems. IEEE Trans Ind Electron 2010;57:963–8. <https://doi.org/10.1109/TIE.2009.2038404>.
- [37] Dasgupta S, Mohan SN, Sahoo SK, Panda SK. Lyapunov function-based current controller to control active and reactive power flow from a renewable energy source to a generalized three-phase microgrid system. IEEE Trans Ind Electron 2013;60:799–813. <https://doi.org/10.1109/TIE.2012.2206356>.
- [38] Wang X, Li YW, Member S, Blaabjerg F. Virtual-Impedance-Based Control for Voltage-Source and Current-Source Converters. IEEE Trans Power Electron 2015;30:7019–37. <https://doi.org/10.1109/TPEL.2014.2382565>.
- [39] Chandorkar MC, Divan DM. Decentralized Operation of Distributed UPS Systems. Proc Int Conf Power Electron Drives Energy Syst Ind Growth 1996. <https://doi.org/10.1109/PEDES.1996.539675>.
- [40] Gao F, Kang R, Cao J, Yang T. Primary and secondary control in DC microgrids : a review. J Mod Power Syst Clean Energy 2019;7:227–42. <https://doi.org/10.1007/s40565-018-0466-5>.
- [41] Tayab UB, Azrik M, Roslan B, Hwai LJ, Kashif M. A review of droop control techniques for microgrid. Renew Sustain Energy Rev 2017;76:717–27. <https://doi.org/10.1016/j.rser.2017.03.028>.
- [42] Gao F, Bozhko S, Costabeber A, Patel C, Wheeler P, Member S, et al. Comparative Stability Analysis of Droop Control Approaches in Voltage Source Converters-Based

- DC Microgrids. IEEE Trans Power Electron 2016;32:2395–415. <https://doi.org/10.1109/TPEL.2016.2567780>.
- [43] Bunker KJ, Weaver WW. Optimal Multidimensional Droop Control for Wind Resources in DC Microgrids 2018;11. <https://doi.org/10.3390/en11071818>.
- [44] Crawley DB, Lawrie LK, Winkelmann FC, Buhl WF, Huang YJ, Pedersen CO, et al. EnergyPlus : creating a new-generation building energy simulation program 2001;33.
- [45] Ridley RB. A More Accurate Current-Mode Control Model 2015. <https://doi.org/10.13140/RG.2.1.2802.4164>.
- [46] Ridley RB. A New Small-Signal Model for Current-Mode Control 1999.
- [47] Brown AR. Topics in the Analysis, Measurement, and Design of High-Performance Switching Regulators 1981.
- [48] Selvakumar S, Madhusmita M, Koodalsamy C, Simon SP, Sood YR. High-Speed Maximum Power Point Tracking Module for PV Systems. IEEE Trans Ind Electron 2019;66:1119–29. <https://doi.org/10.1109/TIE.2018.2833036>.
- [49] Gil-Antonio L, Belem Saldivar-Marquez M, Portillo-Rodriguez O. Maximum power point tracking techniques in photovoltaic systems: A brief review. Int Power Electron Congr - CIEP 2016:317–22. <https://doi.org/10.1109/CIEP.2016.7530777>.